表3 HIV-1感染症の遺伝子治療

抗HIV-1分子	コメント
RNA	
デコイ(decoy)	TatやRevなどの標的配列のデコイを用い，これらによるウイルス複製の増強を阻害する
リボザイム	ウイルス複製に重要なRNA分子を切断して不活化する
アンチセンス	ウイルス複製に重要なmRNAに結合し翻訳を阻害する
siRNA	RNAiによりウイルス複製に重要な細胞(Tsg101，NF-κB，CD4，CCR5など)あるいはウイルス蛋白質(Gag，Pol，Tat，Rev，Vif，Nefなど)の発現を阻害する
蛋白質	
TDN変異蛋白質	結合力はあるが活性がない変異蛋白質(Gag，Tat，Revなど)によって正常ウイルス蛋白質の活性を競合阻害する
細胞内抗体	抗体遺伝子を細胞内で発現させウイルス蛋白質(Env，Tat，Revなど)を不活化する

RNAi: RNA interference(RNA干渉)，siRNA: short interfering RNA，TDN: transdominant negative.

して浮上してきた．ウイルス複製にかかわるウイルスおよび細胞遺伝子(**図1**)をコントロールすることでHIV-1増殖を抑制しようとする方法である．詳細は他の総説に譲るが[7-10]，**表3**に主なものをまとめてみた．このうち，RNAi法は現在最も注目されている遺伝子治療である[11]．

4. 将来展望

HIV-1感染症に対する遺伝子診断技術は基本的に確立されているので，今後の課題はその改良である．特に，ウイルスの変異，進化に迅速に対応できるようなシステムの構築が必要とされるであろう．これに対し，HIV-1/エイズに対する遺伝子治療の将来は明るくない．**表3**に示した抗HIV-1分子はすべて実験室内の細胞レベルでは極めて有効であるが，個体内の標的細胞(HIV-1感染細胞)にいかに効率良く特異的に導入し，発現させるか，この点が大きな未解決の課題となっている．この問題を克服しないかぎり実際の治療には適用困難である．

おわりに

はじめに述べたように，アジア・アフリカ地域でHIV-1感染者は激増している．日本も，先進諸国の中でただ一つ，感染者が増え続けている[12]．HAART法による治療効果は大きいが，根治療法ではなく，抵抗性ウイルスの出現も観察されている．このような状況下では，HIV-1感染を広げないこと，また，個体内や地域に存在するウイルス株を的確に把握することが肝要である．この意味で，HIV-1遺伝子診断は今日ますますその重要性を増しているといえる．

■文　献

1) 足立昭夫：HIVとその遺伝子機能．ヒトレトロウイルス研究の最前線(山本直樹編)，p13-23，シュプリンガー・フェアラーク東京，2002.
2) 足立昭夫ほか：HIV-1, 2．日本臨牀　61(増刊号3)：497-502，2003.
3) 佐藤裕徳，武部　豊：HIVの変異．ヒトレトロウイルス研究の最前線(山本直樹編)，p41-48，シュプリンガー・フェアラーク東京，2002.
4) 照沼　裕：アフリカのAIDS．ヒトレトロウイルス研究の最前線(山本直樹編)，p109-115，シュプリンガー・フェアラーク東京，2002.

5) 今井光信，嶋　貴子：HIV迅速検査．Confronting HIV 2004 no.25，p4-6，ディ・エル・エム・ジャパン，2004.
6) 吉村和久，松下修三：HAARTと潜伏感染．ヒトレトロウイルス研究の最前線(山本直樹編)，p67-74，シュプリンガー・フェアラーク東京，2002.
7) 松下修三：エイズに対する遺伝子治療．感染症の宿主防御機構—理論と実際—(今西二郎編)，p254-263，医薬ジャーナル社，2002.
8) 島田　隆：AIDSの遺伝子治療．AIDS制圧に向けて(高月　清編)，p114-117，医歯薬出版，1996.
9) 明石英雄ほか：RNAiのメカニズム．改訂RNAi実験プロトコール(多比良和誠ほか編)，p16-34，羊土社，2004.
10) 明石英雄ほか：RNAiの応用技術の最新動向—RNAiを用いて何ができるか．改訂RNAi実験プロトコール(多比良和誠ほか編)，p35-44，羊土社，2004.
11) 岡本　尚：RNAi-HIV治療への応用は？ Confronting HIV 2004 no.25，p9-11，ディ・エル・エム・ジャパン，2004.
12) 厚生労働省エイズ動向委員会：国内患者・感染者の届出状況(平成15年エイズ発生動向年報より)．Confronting HIV 2004 no.26，p12-13，ディ・エル・エム・ジャパン，2004.

ELSEVIER

Journal of Neuroimmunology 167 (2005) 108 – 119

Journal of Neuroimmunology

www.elsevier.com/locate/jneuroim

HLA-DRB5*0101 and -DRB1*1501 expression in the multiple sclerosis-associated HLA-DR15 haplotype

Elisabetta Prat [a], Utano Tomaru [a], Lidia Sabater [b], Deric M. Park [a], Rebekah Granger [c], Niels Kruse [d], Joan M. Ohayon [a], Maria P. Bettinotti [e], Roland Martin [a,*]

[a] *Neuroimmunology Branch, National Institute of Neurological Disorders and Stroke, National Institutes of Health, Building 10, Room 5B16, 10 Center DR, Bethesda, MD 20892-1400, USA*

[b] *Laboratory of Immunobiology for Research and Applications to Diagnosis, Centre for Transfusion and Tissue Bank, University Hospital Germans Trias I Pujol, 08916 Badalona, Spain*

[c] *Neuromuscular Diseases Section, National Institute of Neurological Disorders and Stroke, National Institutes of Health, Building 10, 10 Center DR, Bethesda, MD 20892-1400, USA*

[d] *Department of Neurology, University of Würzburg, Josef-Schneider-Str. 11, 97080 Würzburg, Germany*

[e] *Department of Transfusion Medicine/Clinical Center, National Institutes of Health, Building 10, 10 Center DR, Bethesda, MD 20892-1400, USA*

Received 16 November 2004; received in revised form 13 April 2005; accepted 22 April 2005

Abstract

The HLA region, and particularly the DR15 haplotype (containing the two DRB* genes DRB1*1501 and DRB5*0101 and the tightly linked DQ alleles DQA*0102 and DQB1*0602, which together form the DQw6 molecule) in Caucasians, shows the strongest genetic association with multiple sclerosis (MS). In the DR15 haplotype, two β-chains HLA-DRB1*1501 and -DRB5*0101 are co-expressed resulting in two different surface HLA-DR αβ heterodimers, DR2b and DR2a. Most previous studies focused on DRB1*1501, however, both DR2a and DR2b may contribute to MS pathogenesis via antigen presentation to myelin-specific T lymphocytes. We therefore analyzed the expression of the two DR15 genes in various antigen presenting cells (APCs), central nervous system and thymic tissues. Transcript levels were higher for DRB5*0101 in all cell types and tissues. Both HLA-DR heterodimers were expressed at significant levels on the cell surface, where they showed a differential expression pattern in different APCs. They were similarly regulated after stimulation with interferon-γ and interleukin-4. Finally, immunohistochemistry experiments indicated that both molecules were expressed in thymic tissue. Our results encourage future research to investigate the potential functional relevance of both genes for the pathogenesis of MS.
© 2005 Elsevier B.V. All rights reserved.

Keywords: MHC; Multiple sclerosis; Antigen presenting molecules; Antigen presenting cells

1. Introduction

Multiple sclerosis (MS) is considered a T cell-mediated autoimmune disease that is triggered by an as yet unknown foreign agent in genetically susceptible individuals (Martin et al., 1992). Epidemiological and genetic studies, including several whole genome searches (Dyment et al., 2004), provide evidence that MS is genetically complex, i.e. a number of different genes contribute to disease susceptibility (Wandstrat and Wakeland, 2001), and among these, genes of the major histocompatibility complex (MHC; HLA in humans) region show the strongest association. In Caucasian MS patients, the genes of the HLA-DR15 haplotype are the closest associated with disease (Vartdal et al., 1989), and studies of cellular immune responses against myelin antigens (Martin et al., 1992) favor DR alleles as the most relevant.

HLA-DR molecules are heterodimers composed of a highly polymorphic β-chain encoded by DRB1* or DRB3-5* genes associated with a nonpolymorphic α-chain encoded by the DRA1*0101 gene. In most haplotypes, two HLA-DRB genes are expressed, one of the DRB1*

* Corresponding author. Tel.: +1 301 594 9084; fax: +1 301 402 0373.
E-mail address: martinr@ninds.nih.gov (R. Martin).

0165-5728/$ - see front matter © 2005 Elsevier B.V. All rights reserved.
doi:10.1016/j.jneuroim.2005.04.027

locus and one of the loci encoding DRB3*, -4*, or -5*. Consequently, two non-allelic HLA-DR molecules are expressed on the cell surface. In the MS-associated HLA-DR15 haplotype, the two β-chains, HLA-DRB1*1501 and DRB5*0101, together with DR-α result in the two functional surface heterodimers, DR2b (DRA*0101, DRB1*1501) and DR2a (DRA*0101, DRB5*0101) (Vergelli et al., 1997b). In this report, we will use the terms DR2b and DR2a and HLA-DRB1*1501 and -DRB5*0101 interchangeably, even though the latter only refer to the polymorphic DR-β chain genes.

Most studies on the role of HLA-class II molecules in MS examined DRB1*1501, however, some paid attention to the above mentioned co-expression of DR2a and DR2b, and showed that both molecules can serve as restriction elements for myelin basic protein (MBP)-specific T cells (Jaraquemada et al., 1990; Martin et al., 1991; Ota et al., 1990; Pette et al., 1990; Vergelli et al., 1997b) or autoreactive T cells in general. Due to differences in their peptide binding properties, a different spectrum of MBP peptides is presented by DR2a versus DR2b (Vergelli et al., 1997b). Furthermore, in addition to serving as antigen presenting molecules for MBP-specific T cells (Jaraquemada et al., 1990; Vergelli et al., 1997b), the restriction element, i.e. DR2a versus DR2b, may also influence T cell effector functions: DR2a-restricted MBP-specific T cell clones are highly cytotoxic, mediating high-efficiency lysis by perforin, while DR2b-restricted clones mediate low-efficiency lysis via Fas–Fas–ligand interaction (Vergelli et al., 1997a).

It has been described for several HLA DR haplotypes, that the DRB1* gene is differentially expressed from the DRB3*-4*, -5*-encoded beta chain (Berdoz et al., 1987; Cotner et al., 1996; Emery et al., 1993). Furthermore, the level of DR molecule expression is important for the activation of T lymphocytes (Matis et al., 1983), e.g.: increased HLA class II expression could lead to enhanced antigen presentation via increased ligand density (Bontrop et al., 1986), and stronger T cell activation.

In light of the above, we investigated the expression of both DR2a and DR2b. We believe that this data on HLA-DR15 haplotype will encourage future research to investigate the influence of both DR2a and DR2b in MS pathogenesis. We analyzed the mRNA and surface expression of the two genes in peripheral blood mononuclear cells (PBMCs), B cells, monocytes, dendritic cells, activated T cells, cerebrospinal fluid (CSF) cells, and central nervous system (CNS) and thymic tissues obtained from healthy donors (HDs) and MS patients.

2. Materials and methods

2.1. Subjects

The study population consisted of 22 HLA-DR15 positive subjects: 8 HDs and 14 patients with clinically definite MS (7 females and 7 males), of whom 9 were affected by relapsing–remitting MS and 5 by secondary-progressive MS. Seven MS patients were not on therapy, while seven received Interferon β-1a or -1b. MS patients did not receive any immunosuppressive therapy for a period of 3 months prior to the study. Thirteen HLA-DR15 negative subjects, three MS patients and ten HDs, were studied as negative controls. Blood and CSF were obtained under a National Institute of Neurological Disorders and Stroke Institutional Review Board (IRB)-approved protocol. HLA-typing for HLA-A, -B, -C and -DR, -DQ was performed at the Department of Transfusion Medicine, NIH, by molecular HLA typing techniques. The method used was sequence specific primer-PCR amplification of genomic DNA (Player et al., 1996).

2.2. Cell cultures and cell isolation techniques

PBMCs were separated from leukaphereses by density gradient centrifugation (Lymphocyte Separation Medium, Bio Whittaker, Walkersville, MD). Monocytes and B cells were purified from PBMCs, respectively, by adherence to plastic and negative selection using the MACS B cell Isolation Kit (Miltenyi, Auburn, CA). Dendritic cells (DCs) were generated from monocytes using a well-established sequential cytokine treatment as previously described (Thurner et al., 1999). CSF cells were obtained by lumbar puncture from 2 MS patients. Bare lymphocyte syndrome (BLS) cells transfected with HLA-DRB5*0101 (BLS-DR2a), -DRB1*1501 (BLS-DR2b), -DRB1*0401 (BLS-DR4) and -DQB1*0602 (BLS-DQw6) were kindly provided by Dr. W.W. Kwok and Dr. G. Nepom (Benaroya Research Institute, University of Washington, Seattle, WA).

2.3. CNS tissues

Blocks of frozen CNS tissues containing MS lesions were obtained from 7 HLA-DRB1*1501 and -DRB5*0101-positive patients (6 females and 1 male; average duration of disease: 13 years) during autopsy and were kindly provided by Dr. C. Raine (Albert Einstein College of Medicine, New York, USA).

2.4. Thymic tissue samples

Thymic tissue samples were obtained under an IRB-approved protocol (University Hospital "Germans Trias i Pujol", Badalona, Spain) by thoracic surgery at University Hospital Valle de Hebron (Barcelona). Molecular typing was performed on tissue samples to identify HLA-DR15 positive subjects. Thymus 1 was obtained from a 6-year-old subject affected by Down syndrome, thymus 2 from a 69-year-old subject affected by Graves disease, thymus 3 from a 69-year-old subject affected by myasthenia gravis.

2.5. Cytokines and antibodies

Interleukin (IL)-4 and interferon (IFN)-γ were obtained from PeproTech (Rocky Hill, NJ), phytohemagglutinin (PHA) from Sigma (St. Louis, MO) and IFN-β1b from Berlex Laboratories (Richmond, CA). Purified mouse anti-DRB1*1501 (PUH0596) and anti-DRB5*0101 (PUH0427A) IgM monoclonal antibodies (Abs) were purchased from One Lambda Inc. (Canoga Park, CA) under an agreement between One Lambda Inc. and the National Institutes of Health. The same Abs were custom conjugated, respectively, with Alexa Fluor 594 and 488 by Molecular Probes (Eugene, OR) and used for immunofluorescence studies on thymic tissue frozen sections. Anti-DRα Ab (L243) was purchased from ATCC (Rockville, MD) and purified ascites generated by Biocon (Rockville, MD). Additional Abs used during the course of FACS analysis experiments were: goat–anti-mouse IgM and anti-mouse IgG R-Phycoerythrin (PE)-labeled Abs (Jackson ImmunoResearch Laboratories, West Grove, PA), CD11c, CD14, CD86, CD80, CD54, CD1a, CD40, CD19, CD45, CD3 (BD PharMingen, San Diego, CA), CD83 (Immunotech, Marseille, France); isotype controls: mouse IgM, IgG2a, IgG2b, IgG1k, were purchased from Caltag (Burlingame, CA) or from BD PharMingen.

2.6. Reverse transcription and real-time polymerase chain reaction (RT-PCR)

RNA was extracted using RNeasy Mini Kit (Qiagen, Valencia, CA). For each sample, 500 ng of total RNA was reverse-transcribed in 50 μl reaction volume using TaqMan Gold RT-PCR Kit (Applied Biosystems, Foster City, CA) with random hexamers.

The TaqMan 5′ nuclease fluorogenic quantitative PCR assay was performed using the ABI 7700 System (PE Applied Biosystems). Primers and probes for DR2a and DR2b genes were in part modified from Albis-Camps and Blasczyk (1999) or newly designed using Primer Express 1.0 (ABI, Applied Biosystems). Oligonucleotides were placed in polymorphic regions of the genes for maximal specificity. Forward and reverse primers for each set were positioned in exons 1 and 2, respectively, to prevent amplification of contaminating genomic DNA. Primers/probes sequences were the following: DR2a forward primer: 5′ TGGAGGTTCCTACATGGCAAA 3′; DR2a reverse primer: 5′ GCTGTCGAAGCGCAAGTC 3′; DR2a probe: 5′ FAM-TGCGGTTCCTGCACAGAGACATCTATAACC-TAMRA 3′; DR2b forward primer: 5′ AGCTCCCCACT-GGCTTTGT 3′; DR2b reverse primer: 5′ TCCACCGCG-GCCCGCGC 3′; DR2b probe: 5′ FAM-TGCTCCAGGA-TGTCCTTCTGGCTGTT-TAMRA 3′. Primer and probe sequences for the housekeeping gene, human β-actin, were chosen to span exon junctions (Kruse et al., 1997). Since the main goal of this study was to compare the expression levels of DR2a and DR2b, which are co-expressed in the same cell, internal calibration was not essential and human β-actin was considered a suitable calibrator. Real-time PCR assays were conducted using Platinum Quantitative PCR SuperMix-UDG (Gibco BRL, Life Technologies, Carlsbad, CA). $MgCl_2$ and primer and probe concentrations were optimized as described (AppliedBiosystem, 1998).

2.7. DNA plasmid and standard curve preparation

To quantify the mRNA expression of DR2a and DR2b genes, standard curves were prepared using linearized plasmid DNA for HLA-DRB5*0101, HLA-DRB1*1501 and human β-actin (Kruse et al., 1997). Plasmid standard curves were generated performing 10 serial, three-fold dilutions. Each dilution was measured in triplicate in each PCR experiment. The logarithmic value of the initial plasmid target copy number was plotted versus threshold cycle value for each dilution and a linear relationship was detected: in all experiments $R^2 > 0.993$. DR2a, DR2b primer/probe combinations could reliably detect as few as 80 and 40 input copies/reaction, respectively. The efficiencies of the reaction on plasmid DNA and on sample cDNA were comparable, so plasmid materials proved to be a suitable standard for quantitation. The copy number of DR2a, DR2b and β-actin in each sample was calculated based on the respective plasmid standard curves. DR2a and DR2b were then normalized to β-actin.

2.8. Specificity of RT-PCR assay

Based on sequence similarities, we considered that DR2b and DR2a primers/probes were potentially cross-reactive, respectively, with DRB1*1502, *1503, *1506, *1507, *1509 and with DRB5*0104, *0106, *0107 and *0109. Knowing the HLA-typing of donors, we were able to exclude from the study those carrying these alleles. Furthermore, real-time PCR experiments were performed on BLS-DR4, -DQw6 and on 13 cDNA samples obtained from PBMCs of HLA-DR15 negative donors: they were all negative. Additionally, DR2a and DR2b oligonucleotides did not recognize, respectively, DR2b and DR2a transcripts when tested on BLS-DR2b and -DR2a cells and on plasmid material. Control PCR reactions were performed on non-reverse-transcribed RNA to exclude any contamination by genomic DNA. Primers did not share sequence identity with DRB pseudogenes.

2.9. Accuracy of real-time RT-PCR

The intra-assay coefficient of variance (CV)% (i.e.: SD/Average × 100) of threshold cycle values of the DR2a and DR2b real-time PCR assay was between 0.1% and 0.9%. The DR2a/DR2b ratio intra-assay CV% reflecting the variability introduced by the RNA extraction procedure, the RT reaction, and the real-time PCR assay was on average 8.5%. The inter-assay CV% of threshold cycle

values of the PCR reaction performed on cDNA material was 1.3% and 2.4% for DR2a and DR2b, respectively. Similar values were obtained when the reaction was performed on plasmid DNA standards.

2.10. Flow cytometry staining for DR2a and DR2b

Cells were incubated on ice for 30 min with Ab diluted in cold staining buffer (phosphate-buffered saline, 5% fetal bovine serum, 0.1% sodium azide). Before and after incubation, cells were washed twice in staining buffer and immediately analyzed by flow cytometry. Two-color analysis was performed on a FACScan™ using CellQuest software (Becton-Dickinson, San Jose, CA), acquiring 5000 events for each condition based on forward/side scatter parameters.

2.11. Immunofluorescence staining for DR2a and DR2b in tissue sections

Cryostat sections (10 μm) were air dried for 2 h, fixed in ice-cold acetone for 20 min and washed 3 times in PBS. Sections were then incubated for 2 h with Ab in a humidified container. After washings with PBS, sections were mounted in SlowFade Light Antifade Kit with DAPI reagents (Molecular Probes) and viewed with Zeiss Axiovert 200M microscope (Carl Zeiss, NY) using appropriate filters. Single-, double- and triple-color images were digitally captured by a high-resolution CCD camera using AxioVision 3.1 software (Carl Zeiss).

2.12. Specificity and affinity of anti-DR2a and -DR2b antibodies for flow cytometry and immunofluorescence staining

The specificity of anti-DR2a and -DR2b Ab was tested using isotype control Abs and BLS-DR2a, -DR2b, -DR4 and -DQw6 cells, as well as PBMCs obtained from HLA-DR15 negative donors. In particular, for immunofluorescence staining, the Ab specificity was tested using purified isotype control and specific Ab in indirect staining because a directly labeled isotype control Ab was not commercially available. Furthermore, a mixture of BLS-DR2a and -DR2b cells was incubated with the two directly labeled anti-DR2a and -DR2b Abs. The two cell populations were easily distinguishable by the different fluorochromes (Fig. 5b). Ab titrations were conducted to establish saturating concentrations in flow cytometry. As a difference in the affinity between the two Abs may bias the estimation of fluorescence intensity (FI) levels in flow cytometry, L243 (anti-DRα) Ab, a monomorphic anti-DR Ab reacting with DR-alpha and recognizing both DR2a and DR2b, was used to normalize the signals obtained with the two specific Abs. The ratios: specific Ab-mean FI (-MFI) or -geometric MFI

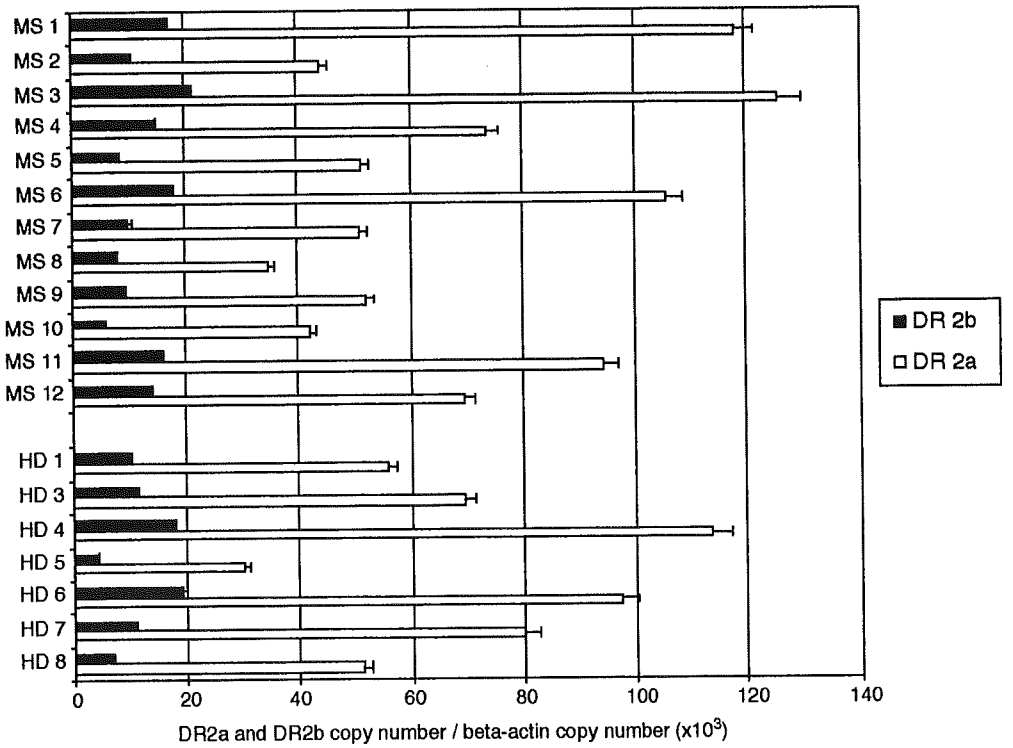

Fig. 1. Relative expression of DR2a and DR2b mRNA in PBMCs obtained from 12 MS patients and 7 HDs. RNA was reverse transcribed and amplified for DR2a and DR2b by real-time PCR. Levels of RNA were normalized to human β-actin. Data are presented as mean of triplicate values ± SD. MS: multiple sclerosis patient, HD: healthy donor.

(-geo.MFI)/L243-MFI or -geo.MFI were calculated for anti-DR2a and -DR2b Ab during the course of repeated experiments on BLS-DR2a or -DR2b cells, respectively. The relative affinity of the anti-DR2a Ab was higher than that of anti-DR2b Ab, and therefore we applied correction factors to all flow cytometry data.

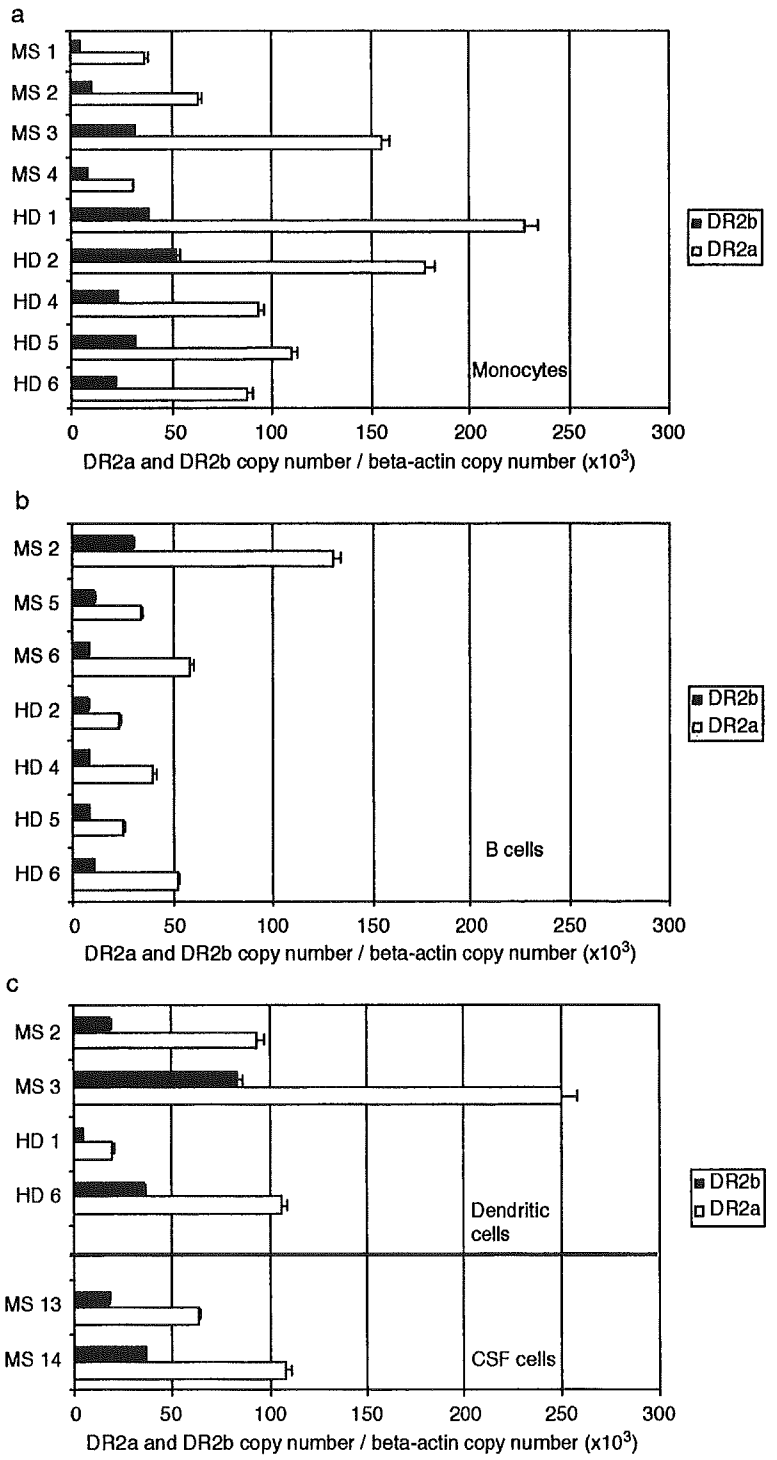

Fig. 2. Relative expression of DR2a and DR2b mRNA in monocytes (a), B cells (b), dendritic cells and CSF cells (c).

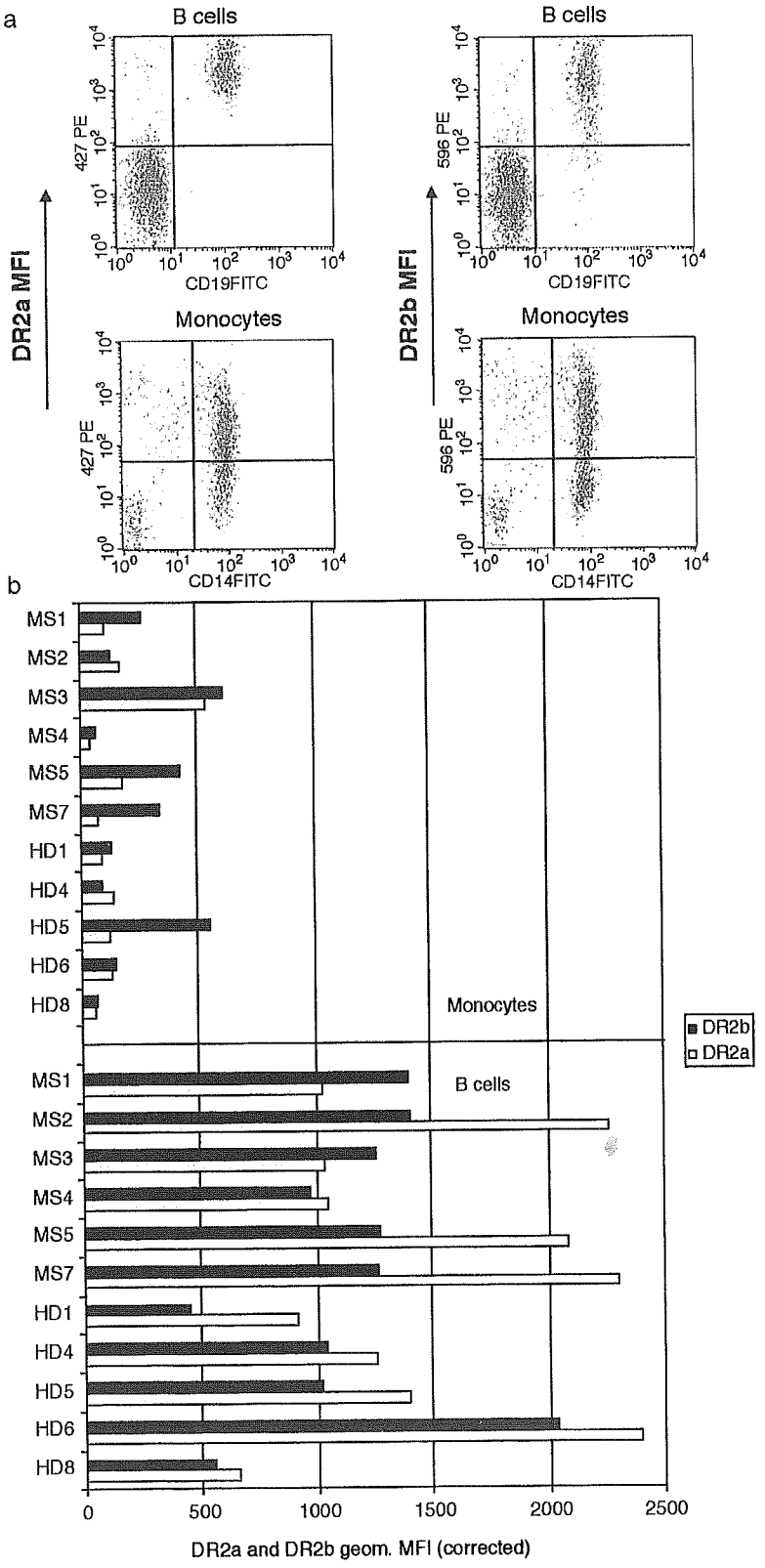

Fig. 3. DR2a and DR2b surface staining on B cells, monocytes and dendritic cells. (a) Representative staining profiles of DR2a and DR2b on B cells (CD19 positive cells) and monocytes (CD14 positive cells). (b) DR2a and DR2b geometric MFI (geom.MFI) values of monocytes and B cells obtained from 6 MS patients and 5 HDs. Geom.MFI values were corrected for the different affinity of the two Abs. (c) DR2a and DR2b MFI values of the same dendritic cells in Fig 2c.

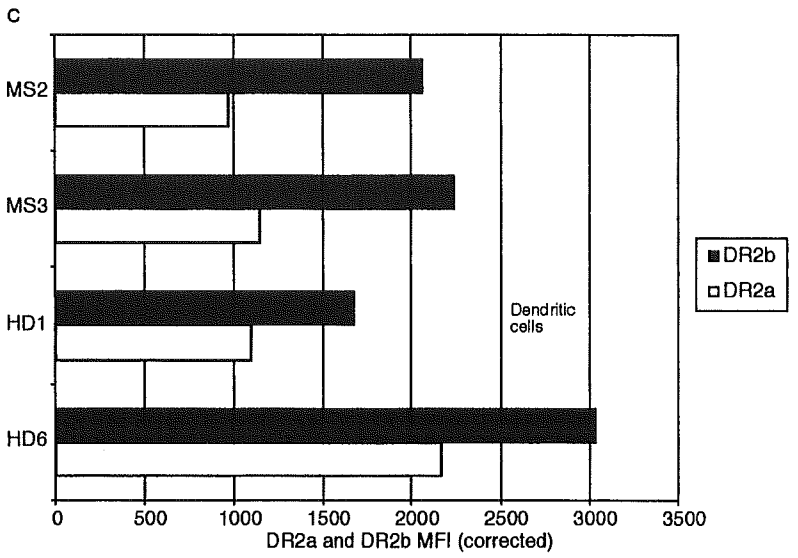

Fig. 3 (*continued*).

2.13. Statistical analyses

Statistical analyses were performed using SigmaStat 2.03 statistical analysis software. Wilcoxon signed-rank test or Wilcoxon rank-sum test was used where appropriate.

Values are expressed as average of DR2a/DR2b transcript or protein levels ratios ± SD.

3. Results

To quantitate the mRNA expression of DR2a and DR2b, we developed a real-time RT-PCR assay and tested its specificity, sensitivity and accuracy as outlined in Materials and methods. Furthermore, we described the methods to assess the specificity and affinity of the two monoclonal Ab that were used to evaluate the surface expression of the two DR molecules by flow cytometry and immunohistochemistry. We subsequently analyzed DR2a and DR2b expression in different APCs and tissues obtained from HDs and MS patients.

3.1. PBMCs

DR2a and DR2b mRNA expression was studied on PBMCs obtained from 12 MS patients and 7 HDs (Fig. 1). DR2a expression was 5 ± 0.8 ($p = 0.001$) times higher than DR2b expression.

3.2. Monocytes, B cells and dendritic cells

Monocytes and B cells were subsequently purified from the PBMCs of a total of 11 donors, 6 MS patients and 5 HDs. On average, transcripts were 4.9 ± 1.6 ($p = 0.004$) (monocytes, Fig. 2a) and 4.3 ± 0.5 ($p = 0.016$) (B cells, Fig. 2b) times higher for DR2a than for DR2b.

Dendritic cells were generated from 2 MS patients' and 2 HDs' monocytes. DR2a mRNA expression was on average 3.7 ± 0.9 times higher than DR2b expression (Fig. 2c).

To study the surface expression of the two molecules, 6 MS patients' and 5 HDs' PBMCs were stained with anti-DR2a and -DR2b Ab. B cell and monocyte populations were identified by gating on CD19+ and CD14+ cells, respectively. As shown in a representative experiment in Fig. 3a, all B cells expressed DR2a at high levels, while DR2b expression varied in intensity across the cell population. In monocytes, the expression varied widely for both alleles, in particular for DR2b. In light of this distribution pattern, we considered that the geometric MFI (geo.MFI) was the best parameter to compare DR2a and DR2b expression in B cells and monocytes. Both DR2a and DR2b were expressed at significant levels on the surface of B cells and monocytes. However, the DR2a geo.MFI value was higher than that of DR2b in 9/11 donors' B cells, and it was on average 1.3 ± 0.4 ($p = 0.042$) times that of DR2b (Fig. 3b). In monocytes, the geo.MFI value of DR2b was higher than that of DR2a in 9/11 donors, and it was on average 2 ± 0.4 ($p = 0.032$) times the expression of DR2a (Fig. 3b).

Similarly to monocytes, dendritic cells surface expression was 1.8 ± 0.3 times higher for DR2b than for DR2a (Fig. 3c).

When comparing the ratio of DR2b/DR2a expression levels between MS patients and HDs, no differences were observed.

To investigate whether DR2a and DR2b expression was differentially modulated by known MHC inducers, we studied their temporal expression in monocytes and B cells

from both HDs and MS patients upon stimulation with 500 U/ml IFN-γ and 20 ng/ml IL-4, respectively. Titrations were performed and the above IFN-γ and IL-4 doses proved to be the most effective for in vitro experiments. A total of 10 time course (24, 48 and 72 h) experiments were performed. The expression of the two alleles was similarly modulated both at the mRNA and surface level (not shown).

3.3. T cells

As activated T cells are able to express MHC class II molecules and may play a role in antigen presentation in addition to professional APCs, we studied DR2a and DR2b surface expression on activated T cells. PBMCs were incubated with 2.5 μg/ml PHA. After 48 h of incubation, DR2a and DR2b surface expression was evaluated on CD3+ T cells: both molecules were up-regulated in about 65% of T cells and their surface expression was 1.6 times higher for DR2b compared to DR2a (not shown).

3.4. Response to IFN-β

We also wanted to study whether DR2a and DR2b expression can be differentially down-modulated. As previously reported, IFN-β, one approved therapy of MS, down-regulates the MHC class II expression induced by IFN-γ in macrophages, B cells and human glial cells (Fertsch et al., 1987; Inaba et al., 1986; Jiang et al., 1995). Therefore, PBMCs were incubated with IFN-β (1000 U/ml) or IFN-γ (100 U/ml), respectively, or a combination of the two, or medium only. DR2a and DR2b surface expression was studied by flow cytometry in B cells. The treatment with IFN-β resulted in an approximately 40% reduction in both HLA-DR2a and DR2b expression induced by IFN-γ (not shown). We did not observe lower levels of DR2a and DR2b surface expression in MS patients that were treated with IFN-β. This is not surprising since in our in vitro experiment IFN-β was used at concentrations higher than those achievable in vivo.

3.5. Cerebrospinal fluid cells

We analyzed DR2a and DR2b mRNA expression in 2 CSF mononuclear cell samples from MS patients. DR2a was on average 3.2 times higher expressed than DR2b (Fig. 2c).

3.6. CNS tissues

In CNS tissues DR2a mRNA expression was on average 5 ± 1.8 ($p = 0.001$) times higher than that of DR2b (Fig. 4).

3.7. Thymic tissue

The thymus is the central immune organ for cellular immune responses and the site of negative and positive selection. As thymic expression of DR2a and DR2b may be important for the development of central tolerance, we analyzed the expression of the two molecules in 3 thymic tissue samples. DR2a mRNA expression was on average 3.5 ± 0.5 times higher than that of DR2b (Fig. 5a). Immunofluorescence staining on frozen sections obtained from the same 3 thymic tissue samples showed that both alleles were clearly expressed (Fig. 5c, d, e). Further studies are necessary to follow up on the preliminary observation of a differential distribution of DR2a and DR2b surface expression in thymic tissue that could not be

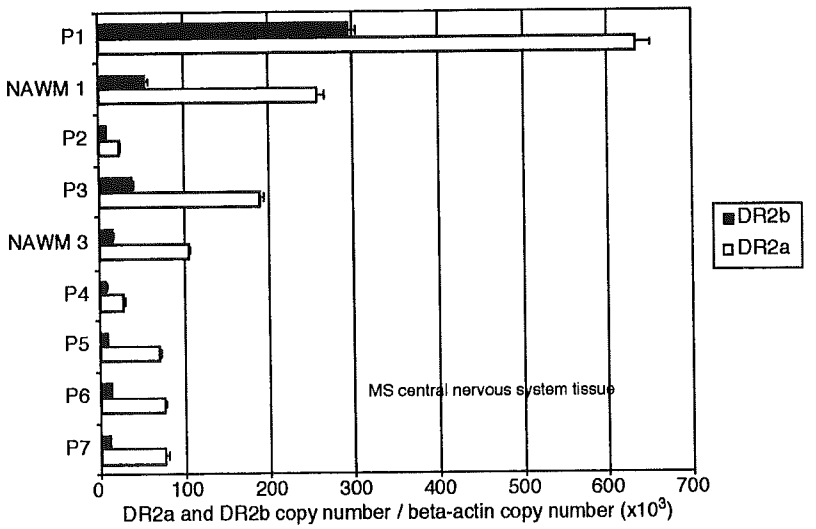

Fig. 4. Relative expression of DR2a and DR2b mRNA in MS lesion containing material obtained from 7 patients. NAWM: normal appearing white matter; P: MS lesion containing material.

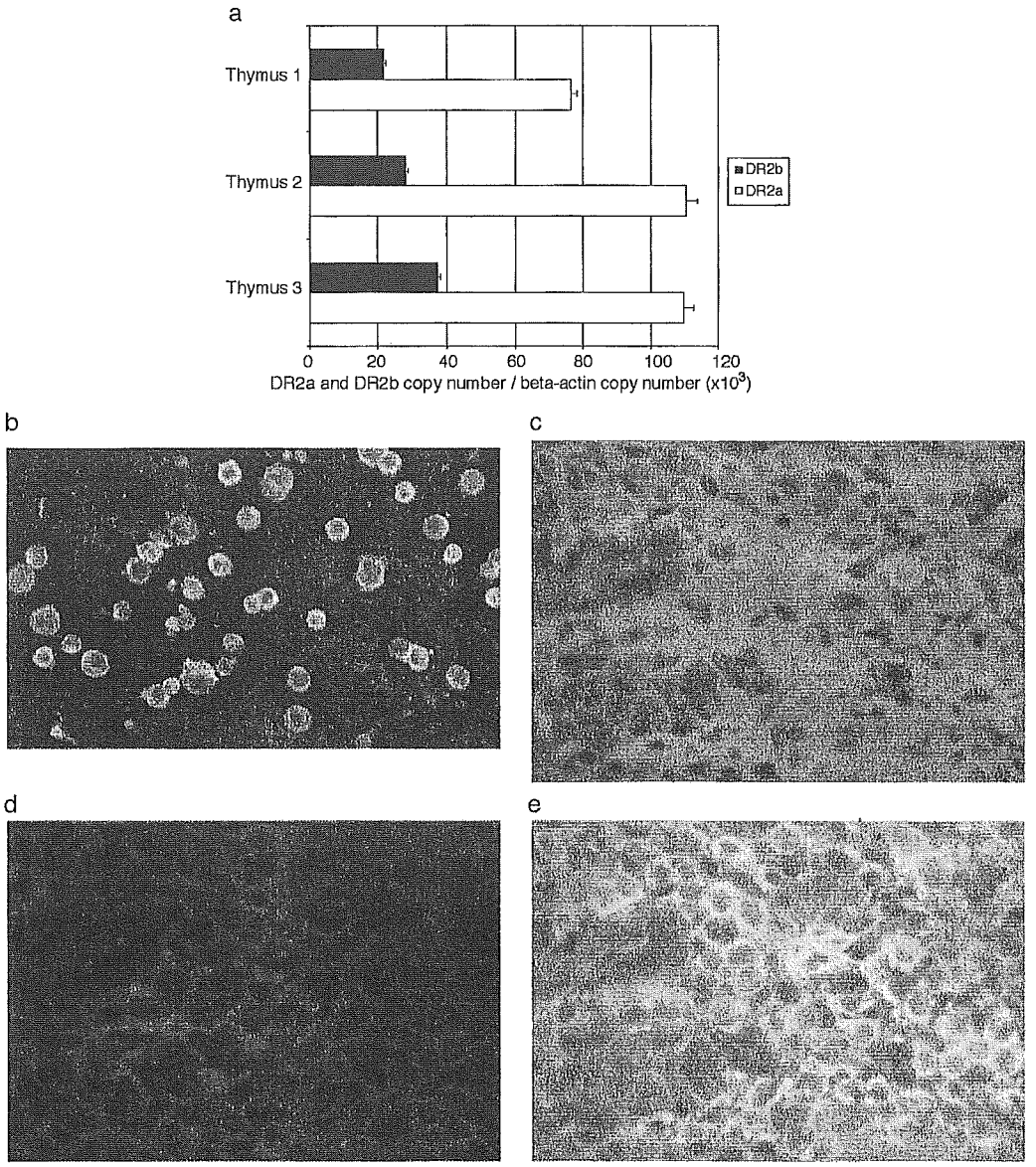

Fig. 5. DR2a and DR2b expression in thymic tissue. (a) Relative expression of DR2a and DR2b mRNA in thymic tissues obtained from 3 donors. (b) A mixture of BLS-DR2a and -DR2b cells was incubated with both Alexa Fluor 488-anti-DR2a Ab (green color) and Alexa Fluor 594-anti-DR2b Ab (red color). The two cell populations were easily distinguishable by the different fluorochromes. (c, d, e) Representative immunofluorescence staining of thymic tissue showing that both molecules were clearly expressed. The section was incubated with Alexa Fluor 488-anti DR2a Ab (c) and with Alexa Fluor 594-anti -DR2b Ab (d). (e) represents the dual image.

studied in more detail with the limited amount of tissue available.

4. Discussion

HLA-class II molecules have been associated with numerous autoimmune diseases (Nepom and Erlich, 1991; Ridgway and Fathman, 1998; Sawcer et al., 2002), and there are several hypotheses that may explain how they could contribute to autoimmunity (Ridgway and Fathman, 1998): (1) Via preferential presentation of certain peptides (e.g. derived from an autoantigen such as MBP) or through presentation of a limited set of peptides and thus less efficient positive or negative thymic selection (e.g. IA^{NOD}) (Nepom and Kwok, 1998). (2) Amino acid sequences of the HLA-DR molecule, which are abundant in the processing compartments, may serve as a mimic for autoantigens (Baum, 1995). (3) The level of MHC/peptide ligand density can influence the functional differentiation of T cells, i.e. into Th1- or Th2-type cells (Constant and Bottomly, 1997). (4) Finally, the two DR-β chains may be expressed

differentially in different cells (e.g. B cells and DCs) and tissues (e.g. in the thymus or the target organ such as brain in MS) and thus may be important for shaping the T cell repertoire or enhancing local T cell activation.

According to the above considerations as to how HLA-class II alleles may impact on T cell-mediated autoimmunity, it is an important step to understand their expression at the mRNA and protein level in disease-relevant cells and tissues.

Even though both DRB5*0101 and DRB1*1501 are expressed in the MS-associated HLA-DR15 haplotype, more attention has been dedicated to DRB1*1501. This may in part be due to the majority of previous reports showing that in various haplotypes DRB1* gene products are expressed at 3–4 times higher levels than the co-expressed DRB3*-4* gene (Berdoz et al., 1987; Cotner et al., 1996; Emery et al., 1993; Stunz et al., 1989).

In agreement with the above-cited studies, a differential mRNA expression in the HLA-DR15 haplotype is described here, however transcripts of the DRB5*0101-encoded allele were more abundant than those of DRB1*1501. One other study also found that the promoter activities of DRB1*03, DRB1*04 and DRB1*07 were lower than the activities of DRB3* and DRB4* promoters (Louis et al., 1994). While some of the discrepancies may be attributable to differences in methods, we believe that our highly specific and sensitive quantitative PCR technique allowed for accurate detection of mRNA levels for DRB1*1501 and DRB5*0101 and that DRB5*0101 mRNA expression is indeed higher than DRB1*1501 in the DR15 haplotype.

In light of the importance of surface protein expression and given that the regulation of individual class II molecules in a tissue-specific manner could play a role in the development of autoimmunity (Berdoz et al., 1987), we studied the surface expression of DRB1*1501 versus DRB5*0101 on monocytes, B cells, dendritic cells, activated T cells and thymic tissues. We found that both molecules were expressed at substantial levels on the surface of various cell types. However, DR2a surface expression was slightly higher than DR2b expression on B cells, while on monocytes, dendritic cells and T cells, DR2b tended to be dominant. Their expression was similarly modulated upon activation of B cells and monocytes by IL-4 and IFN-γ? and down-modulated in B cells by IFN-β. Further, immunohistochemistry experiments indicated that both molecules were expressed in thymic tissue.

DR2 molecule surface expression was studied in B cells and monocytes by flow cytometry, staining PBMCs with anti-CD19 and -CD14 antibodies to gate on each cell population. Therefore, the staining conditions were comparable in B cells and monocytes and cannot account for the observed differential surface expression. As described, transcript levels for DRB5*0101 were higher in all APCs. The observation of a differential DR2a and DR2b surface expression pattern in B cells versus monocytes/dendritic cells merits further investigation and may be due to cell type-specific post-transcriptional regulation. Indeed, it is known that post-transcriptional regulation can contribute to a balanced expression of MHC class II genes (Caplen et al., 1992; Del Pozzo et al., 1999). In B cells, DR2a was expressed at higher levels than DR2b both at the transcript and protein level. However, the difference between DR2a and DR2b surface protein levels was less pronounced. This may be due to limiting DR α-chain expression levels (Czerwony et al., 1999), or alternatively, there may be a ceiling to the total number of DR molecules that can be expressed at the surface. In this regard, it would be of interest to analyze in parallel, as we did in our report, both the transcript and protein expression of specific MHC class II genes in other haplotypes. The differential expression of DR2a and DR2b in different cell types suggests that there are differences in regulation of the two alleles, and this could apply to both resting state and under cytokine stimulation. However, based on current knowledge, we consider it unlikely that the sequential cytokine treatment used to generate DCs may differentially alter the expression pattern of the two genes/molecules. Exposure to interleukin-4 did not differentially regulate the expression of the two genes in the B cell population.

While we found no difference between MS patients and HDs when comparing mRNA and surface expression for the two genes, we believe that the data that we provide on HLA-DR15 haplotype has long been a gap in our knowledge with respect to the more complex patterns of HLA expression in humans compared to mice and encourages future research to investigate the influence of both DR2a and DR2b in MS pathogenesis.

As stated above, MHC molecules may contribute to autoimmunity by their role in antigen presentation. In this regard, both DR2a and DR2b molecules serve as restriction elements for HLA-DR15-restricted-MBP-specific-T cell lines (Pette et al., 1990; Vergelli et al., 1997b). MBP epitopes contained in the immunodominant C-terminal region are uniquely restricted by DR2a, while the immunodominant middle epitope MBP (81–99) is recognized by T cells in the context of both DR2a- and DR2b molecules. Furthermore, a previous study demonstrated that DR2a-restricted MBP-specific T cell clones are highly cytotoxic, mediating high-efficiency lysis by perforin, while DR2b-restricted clones mediate low-efficiency lysis via Fas–Fas–ligand interaction (Vergelli et al., 1997a). The overall comparable levels of surface expression of the two molecules support a role of both alleles in the above mentioned immune functions.

Besides serving as the antigen-presenting molecule to T cells in the periphery, MHC molecules and their expression levels are relevant to the processes of negative and positive selection in the thymus and thus for establishing tolerance to self antigens and preventing autoimmunity. Thymic negative and positive selection could be influenced by differences in the relative expression levels of MHC alleles. Here, we demonstrate that both alleles are expressed in thymi of

DR15-positive individuals, but at present we cannot distinguish whether there is a differential expression of either allele on certain subtypes of thymic cells.

As a further level of complexity, it has been shown that T cells can recognize two different peptides together with two different MHC-class II molecules (Brock et al., 1996; Zhao et al., 1999). In the specific context of MS, a humanized transgenic mouse system for experimental autoimmune encephalomyelitis, a model for MS, allowed the identification of an Epstein–Barr virus peptide that was recognized by encephalitogenic T cells in the context of DR2a, and the same T cell receptor responded to an MBP peptide in the context of DR2b (Lang et al., 2002).These observations broaden the previous concepts on molecular mimicry even further and indicate that a T cell that has been positively selected by one MHC allele and a certain self peptide in the thymus may recognize foreign antigens and/or autoantigens in the periphery in the context of two MHC class II alleles that are co-expressed in the same DR haplotype. Our thymic expression studies indicate that both DR2a and DR2b are available for such cross-reactivity and unpublished data from our laboratory with combinatorial peptide libraries show that these phenomena are probably more frequent than the general concept of MHC restriction of T cells would suggest (Gran, Sospedra et al., unpublished results).

Finally, it was demonstrated that in MS lesions HLA-DR2b molecules were able to present the MBP (85–99) peptide (Krogsgaard et al., 2000). Our findings demonstrate that DR2a transcripts are expressed in MS brain lesions as well as or higher than DR2b. In this regard, it would be interesting to investigate the expression of DR2a protein as well as DR2a-MBP peptide complexes in MS lesions.

In conclusion, we demonstrate that DRB5*0101 transcripts are more prevalent in all cells and tissues and that both DR2a and DR2b are expressed at substantial and largely comparable levels on the surface of various cells. Further studies are needed to establish whether the differential expression on various APCs plays a role during selection processes in the thymus, peripheral immune cells, or the target organ, i.e. the CNS in MS. There is however, no doubt that future MS research should investigate the potential relevance of both genes in the pathogenesis of MS.

Acknowledgments

Elisabetta Prat was supported by a postdoctoral fellowship from the US National Multiple Sclerosis Society. We thank Dr. Ricardo Pujol-Borrell (Badalona, Spain) for kindly providing thymic tissues and advice on the analysis, Dr. Eduard Palou (Badalona, Spain) for tissue typing, Dr. William W. Kwok (Seattle, WA) and Dr. G. Nepom (Seattle, WA) for kindly providing HLA-DRB1*1501 and -DRB5*0101 plasmids and BLS cells, Dr. Cedric S. Raine for CNS tissues, Deborah Kauffman and James W. Naegle (DNA Sequencing Facility, NINDS, NIH). Anti-DR2a and -DR2b Ab were kindly provided by Dr. Jar-How Lee at One Lambda Inc. (Canoga Park, CA).

References

Albis-Camps, M., Blasczyk, R., 1999. Fluorotyping of HLA-DRB by sequence-specific priming and fluorogenic probing. Tissue Antigens 53, 301–307.

AppliedBiosystem, 1998. ABI PRISM 7700 Sequence Detection System. User's Manual, pp. D.20–D.21.

Baum, H., 1995. Mitochondrial antigens, molecular mimicry and autoimmune disease. Biochim. Biophys. Acta 1271, 111–121.

Berdoz, J., Gorski, J., Termijtelen, A., Dayer, J., Irle, C., Schendel, D., Mach, B., 1987. Constitutive and induced expression of the individual HLA-DR β and α chain loci in different cell types. J. Immunol. 139, 1336–1341.

Bontrop, R., Ottenhoff, T., Van Miltenburg, R., Elferink, D., De Vries, R., Giphart, M., 1986. Quantitative and qualitative differences in HLA-DR molecules correlated with antigen-presentation capacity. Eur. J. immunol. 16, 133–138.

Brock, R., Wiesmüller, K.H., Jung, G., Walden, P., 1996. Molecular basis for the recognition of two structurally different major histocompatibility complex/peptide complexes by a single T-cell receptor. Proc. Natl. Acad. Sci. U. S. A. 93, 13108–13113.

Caplen, I.I.S., Salvadori, S., Gansbacher, B., Zier, K.S., 1992. Post-transcriptional regulation of MHC class II expression in human T cells. Cell. Immunol. 139, 98–107.

Constant, S.L., Bottomly, K., 1997. Induction of Th1 and Th2 CD4+ T cell responses: the alternative approaches. Annu. Rev. Immunol. 15, 297–322.

Cotner, T., Charbonneau, H., Mcllins, E., Pious, D., 1996. mRNA abundance, rather than differences in subunit assembly, determine expression of HLA-DRβ1 and DRβ3 molecules. J. Biol. Chem. 264, 11107–11111.

Czerwony, G., Alten, R., Gromnica-Ihle, E., Hagemann, D., Reuter, U., Sorensen, H., Muller, B., 1999. Differential surface expression of HLA-DRB1 and HLA-DRB4 among peripheral blood cells of DR4 positive individuals. Hum. Immunol. 60, 1–9.

Del Pozzo, G., Ciullo, M., Guardiola, J., 1999. Regulation of HLA class II gene expression: the case for posttranscriptional control levels. Microbes Infect. 1, 943–948.

Dyment, D.A., Ebers, G.C., Sadovnick, A.D., 2004. Genetics of multiple sclerosis. Lancet Neurol. 3, 104–110.

Emery, P., Mach, B., Reith, W., 1993. The different level of expression of HLA-DRB1 and -DRB3 genes is controlled by conserved isotypic differences in promoter sequence. Hum. Immunol. 38, 137–147.

Fertsch, D., Schoenberg, D.R., Germain, R.N., Tou, J.Y.L., Vogel, S.N., 1987. Induction of macrophage Ia antigen expression by rIFN-γ and down-regulation by IFN-α/β and dexamethasone are mediated by changes in steady-state levels of Ia mRNA. J. Immunol. 139, 244–249.

Inaba, K., Kitaura, M., Kato, T., Watanabe, Y., Kawade, Y., Muramatsu, S., 1986. Contrasting effect of α/β and γ-interferons on expression of macrophage Ia antigens. J. Exp. Med. 163, 1030–1035.

Jaraquemada, D., Martin, R., Rosen-Bronson, S., Flerlage, M., McFarland, H.F., Long, E.O., 1990. HLA-DR2a is the dominant restriction molecule for the cytotoxic T cell response to myelin basic protein in DR2Dw2 individuals. J. Immunol. 145, 2880–2885.

Jiang, H., Milo, R., Swoveland, P., Johnson, K.P., Panitch, H., Dhib-Jalbut, S., 1995. Interferon β-1b reduces interferon γ-induced antigen-presenting capacity of human glial and B cells. J. Neuroimmunol. 61, 17–25.

Krogsgaard, M., Wucherpfennig, K.W., Cannella, B., Hansen, B.E., Svejgaard, A., Pyrdol, J., Ditzel, H., Raine, C.S., Engberg, J., Fugger, L., 2000. Visualization of myelin basic protein (MBP) T cell epitopes in multiple sclerosis lesions using a monoclonal antibody specific for the

human histocompatibility leukocyte antigen (HLA)-DR2-MBP 85–99 complex. J. Exp. Med. 191, 1395–1412.

Kruse, N., Pette, M., Toyka, K., Rieckmann, P., 1997. Quantification of cytokine mRNA expression by RT PCR in samples of previously frozen blood. J. Immunol. Methods 210, 195–203.

Lang, H.L.E., Jacobsen, H., Ikemizu, S., Andersson, C., Harlos, K., Madsen, L., Hjorth, P., Sondergaard, L., Svejgaard, A., Wucherpfennig, K., Stuart, D.I., Bell, J.I., Jones, E.Y., Fugger, L., 2002. A functional and structural basis for TCR cross-reactivity in multiple sclerosis. Nat. Immunol. 3, 940–943.

Louis, P., Vincent, R., Cavadore, P., Clot, J., Eliaou, J., 1994. Differential transcriptional activities of HLA-DR genes in the various haplotypes. J. Immunol. 153, 5059–5067.

Martin, R., Howell, M.D., Jaraquemada, D., Flerlage, M., Richert, J., Brostoff, S., Long, E.O., McFarlin, D.E., McFarland, H.F., 1991. A myelin basic protein peptide is recognized by cytotoxic T cells in the context of four HLA-DR types associated with multiple sclerosis. J. Exp. Med. 173, 19–24.

Martin, R., McFarland, H.F., McFarlin, D.E., 1992. Immunological aspects of demyelinating diseases. Annu. Rev. Immunol. 10, 153–187.

Matis, L.A., Glimcher, L.H., Paul, W.E., Schwartz, R.H., 1983. Magnitude of response of histocompatibility-restricted T-cell clones is a function of the product of the concentrations of antigen and Ia molecules. Proc. Natl. Acad. Sci. U. S. A. 80, 6019.

Nepom, G.G., Erlich, H., 1991. MHC class-II molecules and autoimmunity. Annu. Rev. Immunol. 9, 493–526.

Nepom, G.T., Kwok, W.W., 1998. Molecular basis for HLA-DQ associations with IDDM. Diabetes 47, 1177–1184.

Ota, K., Matsui, M., Milford, E.L., Mackin, G.A., Weiner, H.L., Hafler, D.A., 1990. T-cell recognition of an immunodominant myelin basic protein epitope in multiple sclerosis. Nature 346, 183–187.

Pette, M., Fujita, K., Wilkinson, D., Altmann, D.M., Trowsdale, J., Giegerich, G., Hinkkanen, A., Epplen, J.T., Kappos, L., Wekerle, H., 1990. Myelin autoreactivity in multiple sclerosis: recognition of myelin basic protein in the context of HLA-DR2 products by T lymphocytes of multiple sclerosis patients and healthy donors. Proc. Natl. Acad. Sci. U. S. A. 87, 7968–7972.

Player, M.A., Barracchini, K.C., Simonis, T.B., Rivoltini, L., Arienti, F., Castelli, C., Mazzocchi, A., Belli, F., Parmiani, G., Marincola, F.M., 1996. Differences in frequency distribution of HLA-A2 sub-types between American and Italian Caucasian melanoma patients: relevance for epitope specific vaccination protocols. J. Immunother. 19, 357–363.

Ridgway, W.M., Fathman, C.G., 1998. The association of MHC with autoimmune disease: understanding the pathogenesis of autoimmune diabetes. Clin. Immunol. Immunopathol. 86, 3–10.

Sawcer, S., Maranian, M., Setakis, E., Curwen, V., Akesson, E., Hensiek, A., Coraddu, F., Roxburgh, R., Sawcer, D., Gray, J., Deans, J., Goodfellow, P.N., Walker, N., Clayton, D., Compston, A., 2002. A whole genome screen for linkage disequilibrium in multiple sclerosis confirms disease associations with regions previously linked to susceptibility. Brain 125, 1337–1347.

Stunz, L., Karr, R.W., Anderson, R., 1989. HLA-DRB1 and -DRB4 genes are differentially regulated at the transcriptional level. J. Immunol. 143, 3081–3086.

Thurner, B., Roder, C., Dieckmann, D., Heuer, M., Kruse, M., Glaser, A., Keikavoussi, P., Kampgen, E., Bender, A., Schuler, G., 1999. Generation of large numbers of fully mature and stable dendritic cells from leukapheresis products for clinical application. J. Immunol. Methods 223, 1–5.

Vartdal, F., Sollid, L.M., Vandvik, B., Markussen, G., Thorsby, E., 1989. Patients with multiple sclerosis carry DQB1 genes which encode shared polymorphic amino acid sequences. Hum. Immunol. 25, 103–110.

Vergelli, M., Hemmer, B., Muraro, P., Tranquill, L., Biddison, W.E., Sarin, A., McFarland, H.F., Martin, R., 1997a. Human autoreactive CD4+ T cell clones use perforin- or Fas–Fas–ligand-mediated pathways for target cell lysis. c 158, 2756–2761.

Vergelli, M., Kalbus, M., Rojo, S.C., Hemmer, B., Kalbacher, H., Tranquill, L., Beck, H., McFarland, H.F., De Mars, R., Long, E.O., Martin, R., 1997b. T cell response to myelin basic protein in the context of the multiple sclerosis associated HLA-DR15 haplotype: peptide binding, immunodominance and effector functions of T cells. J. Neuroimmunol. 77, 195–203.

Wandstrat, A., Wakeland, E., 2001. The genetic of complex autoimmune diseases: non-MHC susceptibility genes. Nat. Immunol. 2, 802–809.

Zhao, R., Loftus, D.J., Appella, E., Collins, E.J., 1999. Structural evidence of T cell xeno-reactivity in the absence of molecular mimicry. J. Exp. Med. 189, 359–370.

Chronic graft-versus-host disease-like autoimmune disorders spontaneously occurred in rats with neonatal thymus atrophy

Tomohisa Baba, Akihiro Ishizu, Hitoshi Ikeda, Yukiko Miyatake, Takahiro Tsuji**, Akira Suzuki, Utano Tomaru and Takashi Yoshiki****

Department of Pathology/Pathophysiology, Division of Pathophysiological Science, Hokkaido University Graduate School of Medicine, Sapporo, Japan

Received 27/10/04
Revised 7/4/05
Accepted 22/4/05

[DOI 10.1002/eji.200425789]

We earlier reported that the human T cell leukemia virus type-1 *pX* gene transduced into rat thymic epithelial cells had an impact on biology of the cells. We report here that FW-pX rats born by mating of F344 transgenic rats expressing the *pX* gene without tissue specificity with nontransgenic Wistar rats developed disorders, including atrophy of the thymus, lymphocytopenia, and inflammatory cell infiltration into multiple organs, similar to events in chronic graft-*vs.*-host disease (GVHD). Vanishment of thymic epithelial cells especially in the cortex and marked depletion of CD4 CD8 double-positive thymocytes were evident in the neonatal thymus in these rats. The relative abundance of CD8 compared to CD4 T cells may be related to dominant infiltration of CD8 T cells into the affected organs. Additionally, adoptive transfer of FW-pX splenocytes could induce lymphocytic infiltration into sublethally irradiated wild-type syngeneic recipients. Analysis of the expression level of the Foxp3 gene in peripheral blood mononuclear cells revealed that the numbers of immunoregulatory T cells were less in FW-pX rats than in wild-type rats. The collective evidence suggested that the FW-pX rats spontaneously developed chronic GVHD-like autoimmune diseases, following abortive differentiation of T cells in the thymus in early days of the newborn. This rat model may shed light on the pathogenesis of chronic GVHD and also other systemic autoimmune diseases, the etiology of which is unknown.

Key words: Thymus · Autoimmune disease · Animal model · Chronic GVHD

Introduction

Human T cell leukemia virus type 1 (HTLV-1) is the etiological agent of adult T cell leukemia/lymphoma [1, 2] and other inflammatory diseases including HTLV-1-associated myelopathy/tropical spastic paraparesis [3, 4] and HTLV-1 uveitis [5]. Since Tax (protein product of the *pX* gene of HTLV-1) modulates expression and function of host molecules such as cytokines, cytokine receptors, growth factors, transcription factors, and cell cycle-related proteins, it is considered that the *pX* gene plays major pathogenetic roles in HTLV-1-associated diseases [6, 7].

To investigate the roles of Tax *in vivo*, we established transgenic rat models carrying the *pX* gene [8–10]. Among them, F344 rats expressing the *pX* gene under control of the rat lymphocyte-specific protein tyrosine kinase p56lck proximal promoter (lck-pX rats) fre-

Correspondence: Akihiro Ishizu, Department of Pathology/Pathophysiology, Division of Pathophysiological Science, Hokkaido University Graduate School of Medicine, Kita-15, Nishi-7, Kita-ku, Sapporo 060–8638, Japan
Fax: +81–11–706–7825
e-mail: aishizu@med.hokudai.ac.jp

Abbreviations: **HTLV-1:** Human T cell leukemia virus type 1 · **DP:** Double-positive **SP:** Single-positive · **HSCT:** Hematopoietic stem cell transplantation · **ssDNA:** Single-stranded DNA

* Present address: Section of Pathology, Hakodate Central General Hospital, Hakodate 040-8585, Japan.
** Present address: Department of Medical Microbiology, University College Dublin, Belfield, Dublin 4, Ireland.
*** Present address: Genetic Lab Co. Ltd, Sapporo 060–0009, Japan.

© 2005 WILEY-VCH Verlag GmbH & Co. KGaA, Weinheim

quently developed epithelial thymoma which originated in the medulla [10]. Although we expected that the *pX* gene was exclusively expressed in lymphoid cells, the transgene was actually expressed in systemic organs including thymic epithelial cells in these rats. These findings suggested that the *pX* gene strongly affected the biology of thymic epithelial cells. To determine whether the phenomenon depended on host genetic backgrounds, we mated F344 lck-pX rats with other strains. We found that epithelial thymoma occurred at a high frequency only when lck-pX rats were mated with syngeneic F344 rats, indicating that host genetic factors are critical for tumorigenicity by the *pX* gene. This interesting theme is now under investigation.

In the present study, we focused on a unique phenotype other than epithelial thymoma seen in F1 rats which were born after mating F344 lck-pX with nontransgenic Wistar rats (FW-pX rats), including atrophy of the thymus, lower body weight than of age-matched controls (FW-wt rats), and dermatitis with hair loss. Lymphocytopenia with unrecognizable formation of follicles in LN and the spleen, and inflammatory cell infiltration into multiple organs were also noted in these rats. We considered that the disorders which occurred in FW-pX rats were similar to events in patients with chronic graft-*vs.*-host disease (GVHD) who had undergone hematopoietic stem cell transplantation (HSCT).

Results

Development of phenotype different from epithelial thymoma in FW-pX rats

F344 transgenic rats expressing the HTLV-1 *pX* gene in systemic organs (lck-pX rats) developed epithelial thymoma, suggesting that the *pX* gene strongly affected the biology of thymic epithelial cells [10]. To examine whether the phenomenon depended on host genetic backgrounds, mating of F344 lck-pX rats with other strains was done. Since epithelial thymoma occurred more frequently in male than in female lck-pX rats (reason currently unknown), we used male lck-pX rats for mating in the present study. Male rats in F1 generation from mating lck-pX rats with syngeneic wild-type F344 rats developed epithelial thymoma at a high frequency. On the other hand, male FW-pX rats obtained by mating of male lck-pX rats with female Wistar rats frequently developed disorders other than epithelial thymoma from early days after birth. In these rats, dermatitis with hair loss, lower body weight than of age-matched controls, and atrophy of the thymus were observed (Fig. 1). Out of 29 male FW-pX rats, 26 (90%) showed a similar phenotype, while most females did not. Incidence of the disease was highest in male FW-pX rats, though frequency of the disease in other F1 strains was up to 20% (data not shown).

Fig. 1. Representative photographs of F1 rats (male, 5 weeks of age). The upper and lower photographs show the FW-wt [(male nontransgenic F344) × (female Wistar) F1] and FW-pX [(male F344 lck-pX) × (female Wistar) F1] rat, respectively. FW-pX rats were physically smaller than age-matched FW-wt rats and manifested dermatitis with hair loss (left). In FW-pX rats, atrophy of the thymus was observed (right). Arrows indicate the thymus.

Structural abnormality of the thymus and apoptosis of thymic epithelial cells and CD4 CD8 double-positive thymocytes in neonatal FW-pX rats

To determine how the thymus atrophied in FW-pX rats, neonatal thymus was examined chronologically. Demarcation between the cortex and medulla was missing due to marked depletion of thymocytes in 10-day-old FW-pX thymus (Fig. 2A). In 2-day-old FW-pX thymus, thymocytes were maintained relatively. Thymic epithelial cells positively stained with anti-cytokeratin Ab were diminished in the FW-pX thymus predominantly in the cortex compared to the medulla, while these cells spread like a mesh in 2-, 5-, and 10-day-old control FW-wt rats (Fig. 2B). In the 5-day-old FW-pX thymus, some nuclei of epithelial cells labeled with anti-cytokeratin Ab were positively stained with anti-single-stranded DNA (anti-ssDNA) Ab (Fig. 2C). These were also positive by terminal deoxynucleotidyl transferase-mediated dUTP nick end labeling (TUNEL, data not shown), suggesting that the loss of thymic epithelial cells was caused by apoptosis. Contrarily, in the age-matched FW-wt thymus, most ssDNA-positive cells were cytokeratin-negative thymocytes (Fig. 2C).

The rate of apoptotic thymocytes in the FW-pX thymus was at a significantly high level at 5 (32.1±5.7%) and 10 days of age (13.0±2.1%) compared with findings in the FW-wt thymus (less than 5% at 2, 5, and 10 days of age) (Fig. 3A). In line with these findings, the numbers of viable thymocytes in the FW-pX

© 2005 WILEY-VCH Verlag GmbH & Co. KGaA, Weinheim

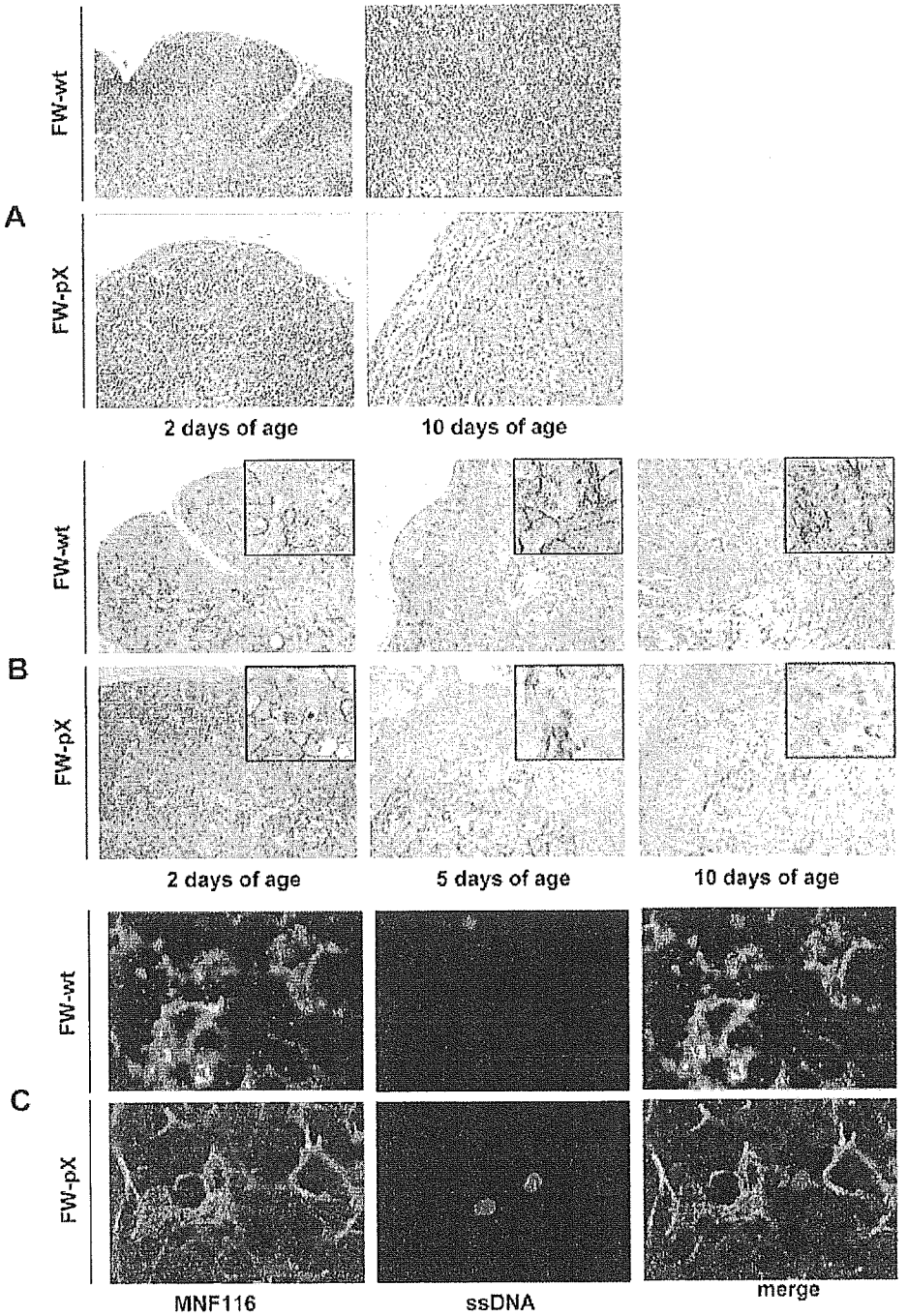

Fig. 2. Structural alteration of the thymus in neonatal FW-pX rats. Photographs show representative findings. (A) H&E staining (original magnification: ×100). (B) Immunostaining for cytokeratin (AE1+AE3) to label thymic epithelial cells (original magnification: ×100). Inset: high-power view of the cortex (×400). (C) Immunofluorescence double staining for cytokeratin (MNF116, green) and ssDNA (A4506, red), using the thymus from 5-day-old rats. The merged image shows that some nuclei of thymic epithelial cells were stained for anti-ssDNA Ab, indicating that thymic epithelial cells are dying by apoptosis in 5-day-old FW-pX rats (lower panels, original magnification: ×400). On the other hand, cells positive for ssDNA do not merge to thymic epithelial cells, indicating apoptosis of thymocytes in FW-wt rats (upper panels, original magnification: ×400).

thymus (5 days of age: $55.4\pm21.8\times10^5$, 10 days of age: $37.6\pm8.4\times10^5$) were significantly less than those of the FW-wt thymus (5 days of age: $365.7\pm67.8\times10^5$, 10 days of age: $1{,}461.8\pm202.7\times10^5$) (Fig. 3B). The rate of CD4 CD8 double-positive (DP) cells in the FW-pX thymus (5 days of age: 7.76%, 10 days of age: 2.77%) was

© 2005 WILEY-VCH Verlag GmbH & Co. KGaA, Weinheim

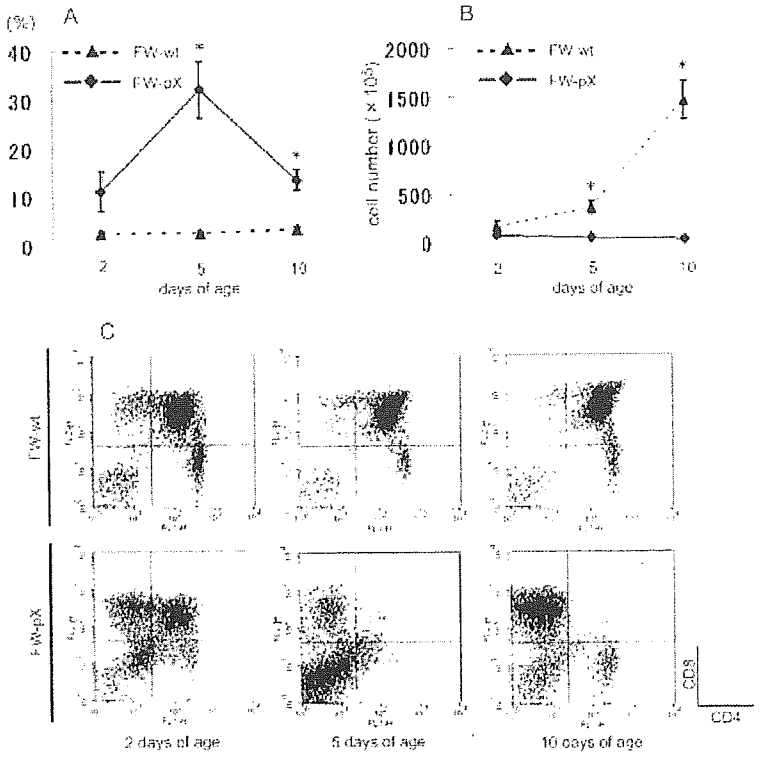

Fig. 3. Analyses of the thymus. (A) Thymocytes were stained with Annexin-V-FLUOS Staining Kit to detect apoptosis, and then analyzed using FACScan. (B) Total number of thymocytes. Viable cell number was counted after Trypan blue staining. (C) Thymocytes from FW-wt (top) and FW-pX rats (bottom) were stained with FITC-conjugated anti-CD4 (OX-35) and PE-conjugated anti-CD8 (OX-8) Ab. In both groups at each time-point, at least three rats were examined. In (A, B), data are represented as mean ± SD (*$p<0.05$). Each panel in (C) shows the representative profile of reproduced results.

significantly low compared with findings in the FW-wt thymus (5 days of age: 80.26%, 10 days of age: 83.87%), suggesting that the most affected cells in the neonatal FW-pX thymus were CD4 CD8 DP thymocytes (Fig. 3C). In addition, CD8 single-positive (SP) cells were noted at a higher ratio than CD4 SP cells in the FW-pX thymus at 2, 5, and 10 days of age.

Alteration of populations of peripheral blood mononuclear cells and abnormality of peripheral lymphoid organs in FW-pX rats

The rate of peripheral T cells reactive with anti-αβ TCR Ab was significantly low in FW-pX rats (4 weeks of age: 25.9±9.2%, 7 weeks of age: 15.0±6.7%) compared with findings in FW-wt rats (4 weeks of age: 49.2±1.0%, 7 weeks of age: 47.7±1.1%) (Fig. 4A). Contrarily, the rate of peripheral myeloid cells reactive with anti-CD11b/c Ab was significantly high in the FW-pX rats (4 weeks of age: 41.4±2.3%, 7 weeks of age: 68.9±11.0%) compared with findings in the FW-wt rats (4 weeks of age: 20.0±0.5%, 7 weeks of age: 20.3±3.2%) (Fig. 4B). The majority (87.2%) of peripheral $CD3^+$ cells were CD8 T cells, while a smaller population (9.8%) was composed of CD4 T cells (Fig. 4C). Expressions of CD25 (predominantly on CD4 T cells), MHC class II, and CD44 were increased on CD4 and CD8 T cells from FW-pX rats (Fig. 4D). On the other hand, expression of CD62L was decreased on CD4 and CD8 T cells from FW-pX rats (data not shown). These findings suggested that peripheral T cells were activated in FW-pX rats.

The absolute numbers of peripheral T cells were significantly decreased with marked depletion of CD4 T cells in FW-pX rats (Table 1). The CD4/CD8 ratio was converse between FW-pX and FW-wt rats, though the numbers of CD8 T cells were also less in FW-pX rats than in FW-wt rats. These findings suggested that CD8 T cells were positively selected or expanded among the small number of T cells in FW-pX rats. Alternatively, dominant defect in the generation of CD4 compared to CD8 T cells may be evident in FW-pX rats. In any case, these findings indicated that T cell differentiation was impaired in FW-pX rats. In contrast to this, higher numbers of peripheral myeloid cells were evident in FW-pX rats than in FW-wt rats. In LN and the spleen in the FW-pX rats, follicular structures were missing due to marked depletion of lymphocytes (Fig. 5).

Inflammatory cell infiltration into multiple organs in FW-pX rats

In FW-pX rats, inflammatory cell infiltration was evident in multiple organs including the skin, liver, salivary glands, and heart (Fig. 6A–D). The major cells infiltrating these organs were mononuclear. In the liver and salivary glands, the epithelium of bile and exocrine ducts, respectively, was affected by infiltrating cells.

© 2005 WILEY-VCH Verlag GmbH & Co. KGaA, Weinheim

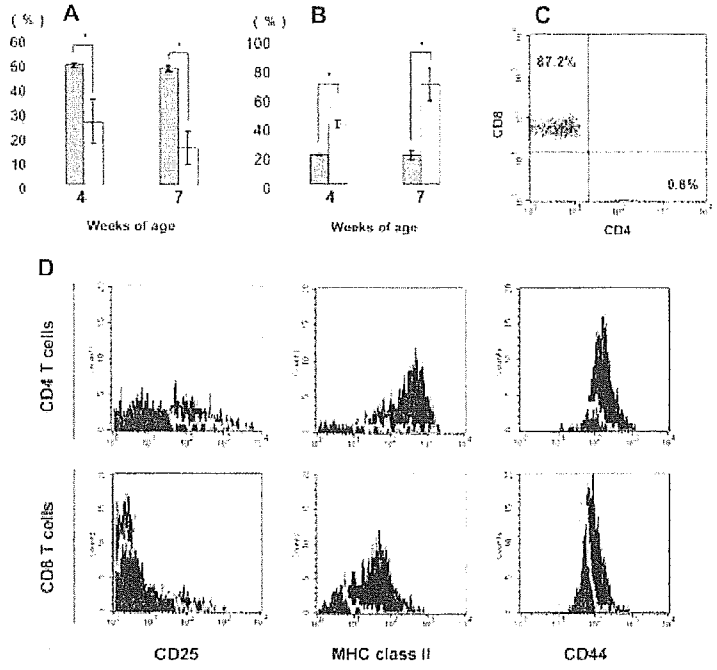

Fig. 4. Population of T and myeloid cells in peripheral blood. (A, B) PBMC were stained with FITC-conjugated anti-αβ TCR (R73) and PE-conjugated anti-CD11b/c (OX-42) Ab, and then analyzed using FACScan. The rate of T cells reactive with R73 (A) and myeloid cells reactive with OX-42 (B) are shown. In both FW-wt (gray bars) and FW-pX rats (white bars) at each time-point, at least three rats were examined. Data are represented as mean ± SD (*$p<0.05$). (C) PBMC were stained with FITC-conjugated anti-CD3 (G4.18), PE-conjugated anti-CD4 (OX-35), and PerCP-conjugated anti-CD8 (OX-8) Ab, and then analyzed using FACScan. Profile was obtained by gating $CD3^+$ cells. (D) PBMC were stained with FITC or PE-conjugated anti-CD4 (OX-35), PerCP-conjugated anti-CD8 (OX-8), and PE or FITC-conjugated Ab for CD25 (OX-9), MHC class II (MRC OX-6), or CD44 (OX-49), and then analyzed using FACScan. CD4 and CD8 SP cells were gated to obtain histograms, respectively. Black and gray histograms represent data from FW-pX and FW-wt rats, respectively. Representative profiles of reproduced results are shown.

Immunohistochemistry revealed that T cells and macrophages dominantly infiltrated into the affected sites (Fig. 6E, F), while B cells and granulocytes were observed to be small in number (data not shown). Approximately a quarter of all the infiltrating $CD3^+$ cells were CD4 T cells, and others CD8 T cells (Fig. 6G, H). In systemic organs, the heart, liver, kidneys, salivary glands, skin, pancreas, and skeletal muscle were susceptible to the inflammatory cell infiltration (Table 2).

Autoimmune response was involved in the development of inflammatory tissue damage in FW-pX rats

To examine the association of affected organs with the transgene, expression level of the *pX* gene was quantified by real-time reverse transcription (RT)-PCR. The *pX* transgene was expressed in all samples examined (data not shown). Among them, the expression was relatively high in the lung and low in the heart, suggesting no significant correlation between the affected organs and expression level of the transgene.

Adoptive transfers of FW-pX splenocytes into sublethally irradiated FW-wt rats were done to determine whether the inflammatory response in FW-pX rats was caused by autoimmune mechanisms. Five days after transplantation, infiltration of mononuclear cells was evident in the liver and heart in recipients (three of five, and one of five cases, respectively) of transferred splenocytes from FW-pX but not FW-wt rats (Fig. 7A, B). Histological aspects were similar to findings in FW-pX rats. Infiltrating cells were mainly composed of T cells and macrophages (Fig. 7C, D).

A possible implication of defect of immunoregulatory T cells in the development of GVHD-like autoimmune diseases in FW-pX rats

Recent studies show that peripheral $CD25^+CD4^+$ immunoregulatory T (T-reg) cells are engaged in inhibiting proliferation of autoreactive T cells, and in the maintenance of immunological self tolerance [11]. It is also shown that Foxp3 is the master gene of T-reg cells in the normal thymus [12, 13]. To assess the contribution of defect of T-reg cells to the development of GVHD-

Table 1. The number of T and myeloid cells in peripheral blood (/μl)[a)]

	T cells	CD4 T cells	CD8 T cells	Myeloid cells
FW-wt	2,319.9±120.3	1,307.6±121.8	704.9±83.9	941.5±70.2
FW-pX	624.7±301.1*	162.6±36.7*	470.4±64.4*	3,709.1±739.7*

a) In both groups, three rats (6 weeks old) were examined. Data are represented as mean ± SD.
*Significant difference ($p<0.05$) between FW-wt and FW-pX rats.

© 2005 WILEY-VCH Verlag GmbH & Co. KGaA, Weinheim

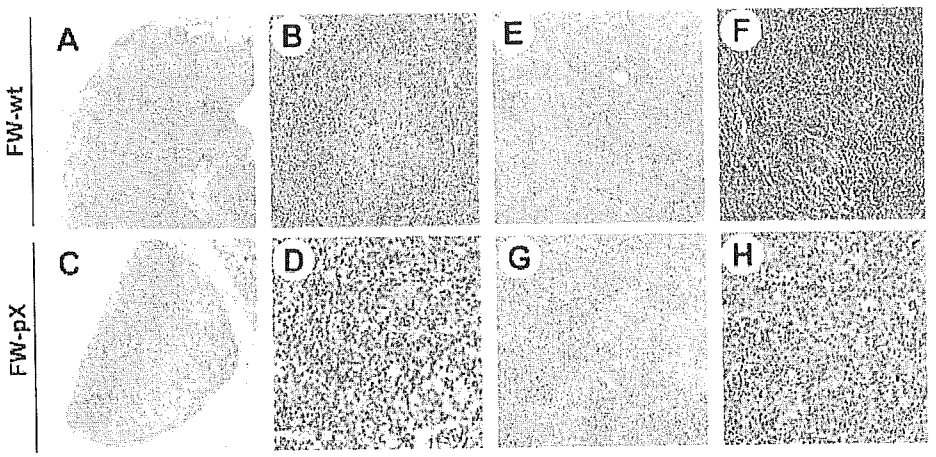

Fig. 5. Structural alteration of peripheral lymphoid organs of FW-pX rats (6 weeks of age). The upper and lower panels show representative findings in FW-wt and FW-pX rats, respectively. Tissue sections of LN (A–D) and the spleen (E–H) were stained with H&E [original magnification: ×20 (A, C, E, G), ×100 (B, D, F, H)]. In both groups, at least three rats were examined.

like autoimmune diseases in FW-pX rats, we compared the expression levels of the Foxp3 gene in PBMC between FW-pX and FW-wt rats, using the quantitative real-time RT-PCR method. When the glyceraldehyde-3-phosphate dehydrogenase (GAPDH) gene was used for standardization, the expression level of the Foxp3 gene was significantly lower in FW-pX rats than in FW-wt rats (Fig. 8). On the other hand, the expression levels appeared to be equivalent between FW-pX and FW-wt rats when the gene for CD3 δ chain was used as a reference. Since the total numbers of PBMC were comparable between FW-pX and FW-wt rats (data not shown), these findings suggested that the numbers of peripheral T-reg cells were less in FW-pX rats than in FW-wt rats, though the proportional alteration in T cells was not evident. The defect of T-reg cells may be associated with the development of GVHD-like autoimmune diseases in FW-pX rats.

Discussion

Chronic GVHD usually appears several months after HSCT and is characterized by weight loss, atrophy of the thymus, reduction in number and function of peripheral T cells, structural alteration of LN and the spleen, and lymphocytic infiltration into systemic organs [14–18]. The susceptible sites of inflammation include the epithelium of bile ducts and salivary glands. Since GVHD occurs after not only allogeneic but also

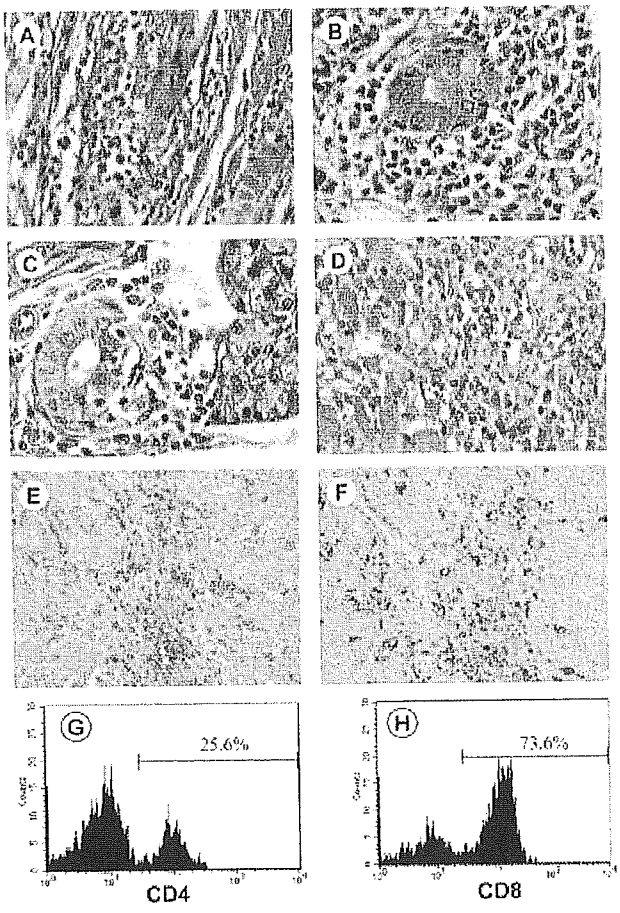

Fig. 6. Inflammatory cell infiltration in systemic organs of FW-pX rats (6 weeks of age). (A–D) Tissue sections from systemic organs were stained with H&E. Photographs show representative findings in the skin (A), liver (B), salivary glands (C), and heart (D). Arrows indicate the epithelium of bile duct (B) and salivary glands (C) affected by lymphocytic infiltration. Tissue sections of the liver were stained with anti-CD3 (CL020AP) (E) and CD68 (ED-1) (F) Ab (original magnification: ×400). Infiltrating cells were eluted from the liver by collagenase digestion, stained with FITC-conjugated anti-CD3 (G4.18) and PE-conjugated anti-CD4 (OX-35), or FITC-conjugated G4.18 and PE-conjugated anti-CD8 (OX-8) Ab, and then analyzed using FACScan. Histograms for CD4 (G) and CD8 (H) were obtained by gating $CD3^+$ cells. Representative data of reproduced results are shown.

© 2005 WILEY-VCH Verlag GmbH & Co. KGaA, Weinheim